Journal of Power Sources 195 (2010) 5493–5500

Contents lists available at ScienceDirect

Journal of Power Sources

journal homepage: www.elsevier.com/locate/jpowsour

Prediction of the effective conductivity of Nafion in the catalyst layer of a proton exchange membrane fuel cell

Kitiya Hongsirikarn, Xunhua Mo, Zhiming Liu, James G. Goodwin Jr.*

Department of Chemical and Biomolecular Engineering, 129 Earle Hall, Clemson University, Clemson, SC 29634-0909, USA

ARTICLE INFO

Article history:
Received 29 January 2010
Received in revised form 23 March 2010
Accepted 24 March 2010
Available online 31 March 2010

Keywords:
Esterification
Proton exchange membrane fuel cell (PEMFC)
Nafion ionomer
Ammonia
Catalyst layer
Effective conductivity

ABSTRACT

In a previous study, a simple acid catalyzed reaction (esterification) was found to predict excellently conductivity of a membrane contaminated with NH_4^+ or Na^+. Since measurement of the conductivity of Nafion in a catalyst layer is problematic, being able to predict this conductivity for various formulations and fuel cell conditions would be advantageous. In this study, the same methodology as before was used to examine the proton availabilities of supported Nafion (Nafion on carbon and on Pt/C), as exists in the catalyst layer used in a PEMFC, during impurity exposure (e.g., NH_3) as a means for prediction of its conductivity. It was found that the effect of NH_3 exposure on the proton composition (y_{H^+}) of supported Nafion was similar to that of N-211 under the same conditions. Determined values of y_{H^+} were then used to estimate the effective conductivity of an ammonium-poisoned cathode layer using the correlation developed and the agglomerate model. The predicted conductivities were matched with the results available in the literature. This technique would be useful for the optimization of catalyst design and for fuel cell simulation, since it provides many benefits over conventional performance test procedures.

1. Introduction

Under fuel cell operation, there are many steps governing overall performance. Depending on operating conditions (e.g., temperature, humidity, current density, etc.), types of material, and also the quality of the fuel and oxidant gases, different steps may limit the performance. Previous studies have shown that in the absence of an impurity, the hydrogen oxidation reaction (HOR) on Pt catalysts occurs rapidly near the interface between the anode catalyst layer and the membrane [1] and the proton transport pathway from Pt sites to the membrane is very short, resulting in negligible effective ionic resistivity at the anode [2]. Therefore, fuel cell performance depends greatly on transport processes in the cathode catalyst layer [3]. However, under some circumstances, where the hydrogen fuel and/or oxidant streams contain contaminants, the rate of the HOR and the oxygen reduction reaction (ORR) on the active catalyst (typically Pt), or the rate of proton transport via the solid electrolyte (generally Nafion) in the ionomer layer and the membrane may be the main determining factor governing the performance of proton exchange membrane fuel cell (PEMFC). For instance, although ammonia is introduced as an impurity at the anode, ammonium diffusion is fast enough for the cathode to be affected [4,5]. It was found that the influence of ammonia adsorption on Pt sites and on HOR at the anode is minimal, but the ionic conductivity of Nafion is significantly affected at even low ppm concentrations [5–7]. Soto et al. [6] found that the increase in membrane resistance can explain only 10% of the voltage loss of PEMFC during an exposure to 1000 ppm NH_3. Thus, the reduction in the membrane conductivity is not the major cause of performance loss of an ammonia-poisoned PEMFC. That is probably due to the complexity at the interface of ionomer and electrode [4–7]. Uribe et al. [7] suggested that the overall performance of the fuel cell could be mainly limited by the efficiency of ionic transport through the Nafion ionomer in the catalyst layer or the kinetics of ORR in the presence of ammonia. However, there is no detailed and quantitative study with experimental support on the effect of foreign cations on the ionic transport within the catalyst layer of a PEMFC.

One reason for the limited number of studies on the fundamental mechanisms is due to the difficulty in conductivity measurement of the Nafion ionomer in a catalyst layer even in the absence of impurity. Up to the present, there is no experimentally measured proton conductivity for this layer that has been reported [8]. Estimated conductivity has been mostly obtained by extrapolating the slope of a polarization plot or by fitting with some parameters in an equivalent circuit [8,9]. The understanding of ionomer conductivity within the active layer is very important because the long-term durability and the performance of large-scale PEMFC operation, where commercial H_2 fuel and air streams

* Corresponding author. Tel.: +1 864 656 6614; fax: +1 864 656 0784.
E-mail address: jgoodwi@clemson.edu (J.G. Goodwin Jr.).

0378-7753/$ – see front matter © 2010 Elsevier B.V. All rights reserved.
doi:10.1016/j.jpowsour.2010.03.074

contain some contaminant cations and material corrosion occurs, could be severely affected by proton starvation within the ionomer phase. Therefore, more studies on the fundamental mechanisms, relating to the ionic migration in the electrode, are required and could be potentially useful for computation and optimization of PEMFC performance.

Previously, the use of a simple acid-catalyzed reaction, esterification, to quantitatively investigate proton availability and to predict the conductivity of a Nafion membrane (N-211) has been validated with experimental results in our laboratory [10]. This methodology provides an alternative means to predict the conductivity of a Nafion membrane for a PEMFC in the presence of contaminants at various conditions without having to carry out conductivity measurements at all those conditions or resort to MEA (membrane electrode assembly) fabrication and fuel cell testing, which are time-consuming and expensive tasks [11–13]. Moreover, unlike other destructive techniques such as elemental analysis, titration, temperature program desorption (TPD), etc., this technique can be used to continuously diagnose the proton availability of the Nafion ionomer during contaminant exposure using only a single sample.

In this study, we further applied esterification (the methanolysis reaction of acetic acid, Eq. (1)),

$$CH_3OH + CH_3COOH \xrightarrow{H^+} H_2O + CH_3COOCH_3 \quad (1)$$

to examine proton composition (y_{H^+}) of supported Nafion (Nafion on a carbon support and on Pt/C, resembling the agglomerates that constitute the catalyst layer in a PEMFC) during impurity (ammonia) exposure. The proton composition (y_{H^+}) is expressed in Eq. (2),

$$y_{H^+} = \frac{C_{H^+}}{\left[C_{H^+}\right]_0} \quad (2)$$

where y_{H^+} and C_{H^+} are the proton fraction and proton concentration of Nafion components, respectively; and $[C_{H^+}]_0$ is the ion exchange capacity of a Nafion component in the fully protonated form. The quantity y_{H^+}, determined under various conditions including ammonia poisoning, was used herein to estimate the effective ionic conductivity of the cathode catalyst layer using the well-known steady-state agglomerate model which was then compared to measurements in the literature.

2. Experimental

2.1. Nafion materials

Two Nafion-containing materials were prepared for this study using the impregnation method. One material had components similar to the catalyst layer in a PEMFC (Nafion supported on Pt/C) and another material contained only Nafion on the carbon support for comparison purposes.

The as-received Nafion ionomer solution (LQ-1105, DuPont, 5 wt.% Nafion) was impregnated on carbon black powder (Vulcan XC-72R, Carbot International) and a commercial 20 wt.% Pt/C (E-TEK) by incipient wetness, since this technique is believed to provide a better contact of the triple phase boundaries between the Nafion, Pt, and carbon support [14–17]. The perfluorosulfonic acid ionomer content in the catalysts was fixed at ~30 wt.% because this Nafion loading has been found to be optimum for PEMFC applications [18–22]. In this study, the ionomer content in the electrode catalyst is defined as: ionomer content (wt.%) = $(W_{ion}/W_{total}) \times 100$, where W_{ion} is the weight of dry ionomer, and W_{total} is the total weight of dry ionomer and support (carbon or Pt/C). After impregnation, the 30 wt.% Nafion on the carbon support (designated as 30-Nfn/C) and the 30 wt.% Nafion on Pt/C (30-Nfn/Pt/C) were dried overnight in an oven at 80 °C in dynamic air flow. The resulting agglomerates were then crushed and screened between sieves (80–230 mesh) before being stored in the dark prior to use.

2.2. Physical characterization

2.2.1. BET surface area

The total surface areas of supported Nafion (30-Nfn/C and 30-Nfn/Pt/C) were determined via the BET method utilizing a Micromeritics ASAP 2001 apparatus. The pore size distribution curves were obtained through the analysis of the nitrogen adsorption and desorption isotherms at 77 K. Prior to the BET measurements, the material was degassed at 5 μm Hg and 110 °C for 4 h.

2.2.2. Ion-exchange capacity (IEC)

The concentrations of proton/acid sites on 30-Nfn/C and 30-Nfn/Pt/C were examined by titration. For a typical titration, a 100 mg of sample was immersed in 0.005 M NaOH (Acros Organics) at room temperature for 2 days under constant shaking. Then, the sample was filtered out and the exchanged solution was back-titrated with 0.005 M HCl (Acros Organics) using phenolphthalein as an indicator. The end point was determined by pH meter at a pH value of 7.

2.2.3. Ammonia analysis

Nafion on different supports (30-Nfn/C and 30-Nfn/Pt/C) after ammonia exposure for a certain period were ion-exchanged with 0.05 M HCl (Acros Organics) at room temperature under constant shaking for at least 7 days. Then, the sample was filtered out from the aliquot. The ammonium concentration in the exchange solution was examined by an ion-selective electrode (ammonia electrode 9512 Thermo Scientific and Orion 4 star pH benchtop meter).

2.3. Esterification measurements

The procedures have been described in more detail elsewhere [10]. Prior to gas-phase esterification, approximately 100 mg of 30-Nfn/C or 30-Nfn/Pt/C was placed between quartz wool plugs in the middle of a differential tubular reactor (ID = 0.7 cm). The sample was pretreated in 100 sccm H_2 at a given humidity, 80 °C, and 1 atm for 3 h. Then, a known amount of reactants (acetic acid (HAc) and methanol (MeOH)), water vapor, and ammonia was introduced to the reactor. The esterification was carried out with an equimolar, low concentration mixture of MeOH and HAc ($P_{MeOH} = P_{HAc} = 0.009$ atm) at a given humidity, 80 °C, and 1 atm in 100 sccm H_2. The reaction activity is defined as the rate of methyl acetate formation (r_{MeOAc}). The concentrations of reactants (MeOH and HAc) and product (MeOAc) in the outlet stream were analysed by a Varian CP-3380 GC equipped with an FID detector and a Varian CPWAX 52CB fused silica capillary column (60 m × 0.53 mm × 1 μm).

3. Results and discussion

3.1. Characterization

Table 1 summarizes the surface acid site concentrations and surface areas of the Nafion samples used in this study. Unexpectedly, the sulfur concentrations in the carbon support (XC-72R) and 20 wt.% Pt/C were rather high (ca. 0.65 wt.% and 0.51 wt.%, respectively). However, this sulfur did not form any significant number of active acid sites. Thus, the acid site concentrations based on sulfur analysis of 30-Nfn/C and 30-Nfn/Pt/C were determined by subtraction of the sulfur content of the support (accounting for its weight fraction) from the total sulfur content. The acid site concentrations

Table 1
Characteristics of the Nafion membrane, supports, and supported Nafion materials.

Sample	Sulfur content[a] (wt.%)	Surface acid site concentration (μmol g^{-1})		BET surface area (m^2 g^{-1})	Average pore size diameter (nm)	Pore volume (cm^3 g^{-1})
		Elemental analysis[a]	Titration[b]			
N-211 [10]	2.96	925	925 ± 17	–	–	–
Carbon support	0.65	0	4.8 ± 0.3	209	14	0.57
30-Nfn/C	1.37	278[c]	265 ± 25	59 ± 3	32 ± 0.3	0.49 ± 0.07
20 wt.% Pt/C support	0.51	0	–	116	24	0.70
30-Nfn/Pt/C	1.23	264[c]	279 ± 19	62 ± 3	28 ± 3	0.40 ± 0.12

[a] From sulfur elemental analysis; experimental error = ±5%.
[b] Ion-exchanged with 0.005 M NaOH at room temperature for 2 days.
[c] The active acid site concentrations for the supported Nafion were determined by subtracting the sulfur content of the support from the total content (0.65 wt.% and 0.51 wt.% for 30-Nfn/C and 30-Nfn/Pt/C, respectively).

obtained from acid–base titration were consistent with the results from sulfur analysis. It can be seen that the site density (per g) of a N-211 membrane was about three times higher than those of 30% Nafion loading on the carbon support or Pt/C (30-Nfn/C and 30-Nfn/Pt/C), as would be expected.

3.2. Esterification activity of supported Nafion (30-Nfn/C and 30-Nfn/Pt/C)

Fig. 1(a and b) shows the activities of 30-Nfn/C and 30-Nfn/Pt/C, respectively, in the presence of 20 ppm NH_3 at different humidities, 1 atm, and 80 °C. The solid line indicates how the activity would have changed if, at 0%RH (where %RH stands for % relative humidity), 100% of ammonia in the gas phase had been absorbed by

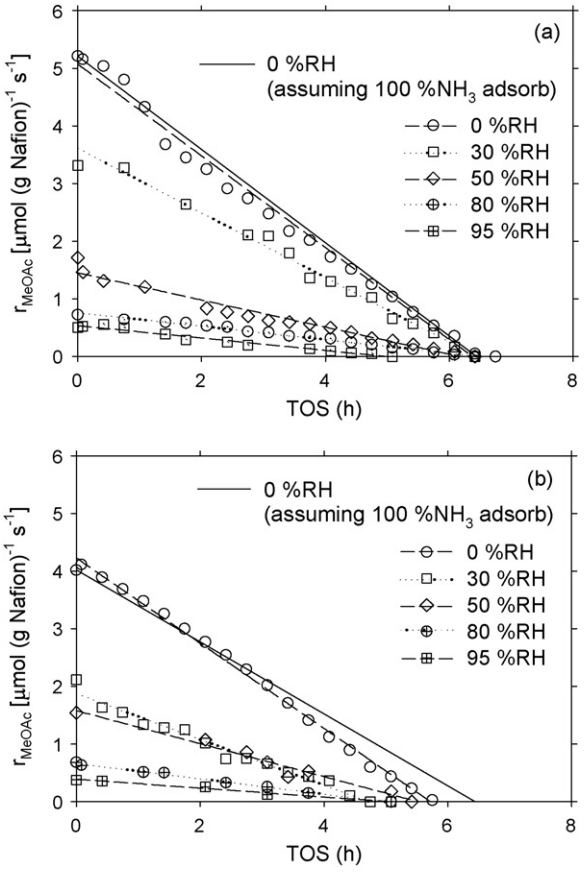

Fig. 1. Esterification activity of supported Nafion in the presence of 20 ppm NH_3 at 1 atm and 80 °C under 100 sccm H_2: (a) 30-Nfn/C, and (b) 30-Nfn/Pt/C. (The solid line represents the theoretical curve assuming that 100% of ammonia flowing through the reactor adsorbs onto the Brønsted acid sites.)

Nafion ionomer, irreversibly poisoning the acid/proton sites. For other humidities, since the total flow and ammonia concentration were kept constant, the time required to fully poison with ammonia would be the same as that at 0%RH (6.4 h). The results indicate that the ionomer/catalyst essentially adsorbed all the ammonia impurity in the gas stream at 0%RH as it passed through the reactor. In this study, the kinetics of activity decrease of 30-Nfn/C and of 30-Nfn/Pt/C were limited in a similar way by the low concentration of ammonia in the gas stream. It can be seen that the activity linearly decreases with time-on-stream (TOS) exposure to ammonia and the initial activity declines with an increase in humidity. These trends are in good agreement with the results for a Nafion membrane (N-211) obtained in our previous work (see Fig. 7(a and b) in Ref. [10]). Table 2 compares the steady-state activities prior to exposure to ammonia of supported Nafion with a N-211 Nafion membrane at various humidities, 1 atm, and 80 °C. It shows that the non-poisoned activities decrease with an increase in humidity for both the Nafion membrane and the supported Nafion. This is because of the competitive adsorption of water vapor with the reactants, the decrease in strength of the Brønsted acid sites, and the reverse hydrolysis of methyl acetate. The explanations for this behaviour have already been discussed in more detail elsewhere [10]. Table 2 also presents the effect of the supports on the esterification activity. It can be seen that, under the same conditions, the activities [μmol (g Nafion)$^{-1}$ s^{-1}] of N-211 compared well with those of 30-Nfn/C and 30-Nfn/Pt/C on a per g Nafion basis, with only some variance. This variation was probably due to the differences in Nafion properties (e.g., dispersity, interaction with support) and in the thermal history during preparation.

From energy-dispersive X-ray spectroscopy (EDS), the Nafion dispersions on 30-Nfn/C and 30-Nfn/Pt/C were similar (data not shown here). The support increases the accessibility of reactants to the Nafion. Thus, the C-supported Nafion (30-Nfn/C) exhibited higher catalytic activity than the Nafion film under the same conditions, as can be seen in Table 2. However, the activity on 30-Nfn/Pt/C was the lowest at all humidities studied. Since esterification was carried out in a H_2 atmosphere, it is likely that acetic acid hydro-

Table 2
Steady-state esterification activity of Nafion samples in the H^+-form at 80 °C[a].

%Relative humidity (%RH)	r_{MeOAc} [μmol (g Nafion)$^{-1}$ s^{-1}][b]		
	N-211 [10]	30-Nfn/C	30-Nfn/Pt/C
0	4.99	5.21	3.79
15	2.94	4.04	–
30	2.72	3.31	2.00
50	1.66	1.98	1.46
65	0.63	1.05	–
80	0.47	0.73	0.64
95	0.24	0.53	0.36

[a] At 1 atm with $P_{MeOH} = P_{HAc} = 0.009$ atm (balance H_2) in a total flow of 100 sccm.
[b] Esterification activity; error = ±5%.

genation occurred on reduced Pt at this condition (0–100%RH, 1 atm, and 80 °C) and caused the decrease in esterification activity. It was found that the selectivity toward methyl acetate was ca. 98% for the 30-Nfn/Pt/C sample, instead of 100% as for the 30-Nfn/C and N-211 samples. We observed trace amounts of ethylene, dimethyl ether, acetaldehyde, and ethanol during esterification on 30-Nfn/Pt/C. These by-products partially consumed acetic acid which was a reactant for esterification and may have also blocked some of the free Nafion sites. This finding is consistent with that reported by Rachmady and Vannice [23] who studied the hydrogenation of acetic acid over reduced Pt. Additionally, it is known that the activity of esterification is affected by the strength of the acid sites [24]. In the vicinity of carbon and Pt/C, the acidity of the acid sites of Nafion may be impacted by the support-Nafion interactions. Also, the properties of Nafion can be influenced by its thermal history [25,26]. The preparation procedures for the Nafion supported materials were significantly different from those for the Nafion membrane [27]. The experimental results imply that differences in Nafion dispersions, interaction with support, side reactions, and heat treatment cause the differences seen in activity for esterification.

Experiments at various conditions (0–95%RH, 1 atm, and 80 °C) were also carried out on the support to clarify the influence of the support on the catalytic activity. Methyl acetate formation on either supports (carbon and Pt/C) was negligible (data not presented here). However, we observed trace amounts of by-products from acetic acid hydrogenation on Pt/C.

3.3. Correlation between esterification activity of the Nafion ionomer and proton composition

Since the determination of y_{H^+} was destructive, a number of samples had to be used for different time-on-streams (TOS). The expressions for the ammonium and proton compositions are as follows:

$$y_{NH_4^+} = \frac{C_{NH_4^+}}{[C_{H^+}]_0} \quad (3)$$

$$y_{H^+} = 1 - y_{NH_4^+} \quad (4)$$

where y_{H^+} and $y_{NH_4^+}$ are the proton and ammonium fractions in a Nafion component, respectively; and $C_{NH_4^+}$ and $[C_{H^+}]_0$ are the ammonium ion concentration and the ion exchange capacity of the Nafion component, respectively.

In Fig. 2(a and b), the esterification activities and the concentrations of free acid/proton sites (y_{H^+}) of a Nafion component for the 30-Nfn/C and 30-Nfn/Pt/C materials in H_2 containing ppm NH_3 and 50%RH at 1 atm and 80 °C are illustrated, respectively.

It can be seen in Fig. 2(a and b) that the catalytic activity decreases with time-on-stream (TOS) accordingly to the decrease in proton concentration in the Nafion ionomer (y_{H^+}) for both supported Nafion materials. Fig. 3 illustrates the normalized esterification activities ($r_{MeOAc,\,Norm.}$, Eq. (5)) of supported Nafion as a function of proton compositions for 50%RH and 80 °C.

$$r_{MeOAc,Norm.} = \frac{(r_{MeOAc,\ y_{H^+}})_t}{(r_{MeOAc,\ y_{H^+}=1})_0} \quad (5)$$

where $(r_{MeOAc,\ y_{H^+}=1})_0$ and $(r_{MeOAc,\ y_{H^+}})_t$ are the catalytic activities of supported Nafion at time-on-stream (TOS) = 0 and t, respectively.

One can see from Fig. 3 that the normalized esterification activities of both 30-Nfn/C and 30-Nfn/Pt/C have a similar linear relationship with proton fraction regardless of the differences in the initial activity, interaction with supports, and side reactions.

The experimental results imply that in the presence of other materials (i.e., alloyed Pt, C support) and other impurities, the acid site/proton concentration of a Nafion polymer can be quantitatively

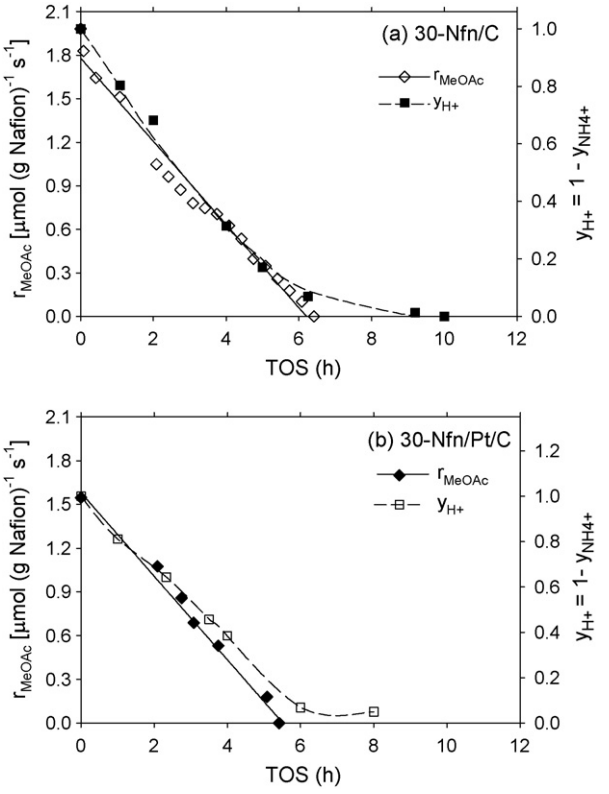

Fig. 2. Relationship of esterification activity to proton fraction of: (a) 30-Nfn/C, and (b) 30-Nfn/Pt/C at 50%RH in the presence of 20 ppm NH_3 and 80 °C. (The maximum ammonium contents of 30-Nfn/C and 30-Nfn/Pt/C were 263 ± 3 and 240 ± 30 µmol g^{-1}.)

investigated by this acid-catalyzed reaction. Unlike a conventional titration method, which is a destructive technique, esterification allows us to study the effect of contaminants on the proton availability of a Nafion component in situ and to continuously monitor using only a single sample the available proton composition during impurity exposure.

3.4. Modified steady-state agglomerate model to predict the overall conductivity of a contaminated catalyst layer in a PEMFC

The effective protonic conductivity is crucial to the performance and optimization of the active layer in PEMFCs [28]. Generally, there

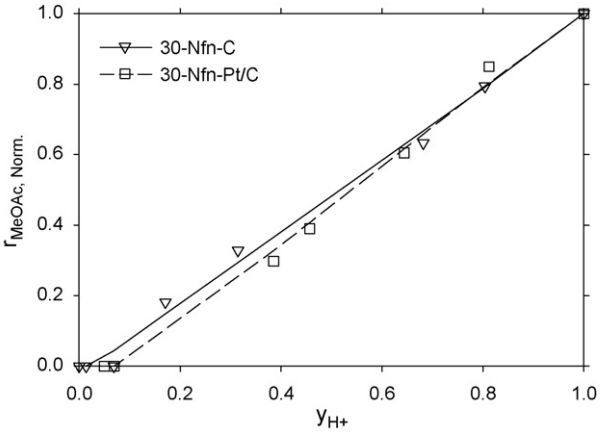

Fig. 3. Relationship of normalized esterification activity ($r_{MeOAc,\ Norm.}$) to proton fraction from Fig. 2(a and b).

are three main approaches to explain the proton transport in a catalyst layer (where three-phase contact exists between ionomer, catalyst, and carbon support): the agglomerate, thin-film, and homogeneous models [29–34]. Among these models, the agglomerate concept is the most popular and the most theoretically based model. It matches very well with experimental data, especially for fuel cell operation at high current density (mass transportation limitations) [31,34–38]. The well-known effective proton conductivity in an active layer has been derived by Jaouen et al. [31] using the steady-state agglomerate model and is as follows:

$$\sigma_{eff}^{cat} = (1-\varepsilon_{cat})\left[1+\frac{(\varepsilon_{agg}-1)}{(1+(\delta/r_{agg}))^3}\right]\sigma \quad (6)$$

$$\sigma_{eff}^{cat} = C\sigma \quad (7)$$

where σ_{eff}^{cat} and σ are the effective conductivity of the catalyst layer (active layer) and the bulk conductivity of the polymer (typically Nafion) fraction in the catalyst layer, respectively; ε_{agg} and ε_{cat} are the volume fractions of the polymer in the agglomerate and of the pores in the catalyst layer, respectively; r_{agg} is the agglomerate radius; δ is the thickness of the polymer film surrounding the agglomerate; and C is a factor depending on the operating conditions and physical properties of the metal(s), support, and ionomer used in the catalyst layer.

It can be seen in Eq. (7) that, in the absence of impurities, the effective conductivity is the product of a constant factor C and the bulk conductivity of the polymer. The factor C depends on the physical properties of the catalyst layer, for example, porosity, radius of the agglomerate, thickness of polymer surrounding the agglomerate, etc. Thus, the factor C can be considered to remain constant during exposure of the ionomer to impurities that do not affect these properties. For the ammonium-poisoned catalyst layer in this study, the factor C was assumed to be constant and the effective conductivity was able to be obtained by knowing the proton composition (y_{H^+}). The correlation of the Nafion conductivity at typical fuel cell operation as a function of ammonium content has been reported in our previous study [27]. Accordingly, the effective conductivity of an ammonium-poisoned catalyst layer can be estimated as follows:

$$\sigma_{eff}^{cat} = C\sigma_{y_{NH_4^+}} \quad (8)$$

$$\sigma_{y_{NH_4^+}} = \frac{A_3}{1+A_1\exp(A_2 y_{NH_4^+})} + A_4 \quad (9)$$

where y_{H^+} and $y_{NH_4^+}$ are the concentrations of protons and ammonium ions in the Nafion polymer obtained from the esterification activity, respectively; $\sigma_{y_{NH_4^+}}$ is the conductivity of the Nafion polymer containing $y_{NH_4^+}$ at 80 °C; and parameters ($A_1 - A_4$) are given in Table 3. The expression for $\sigma_{y_{NH_4^+}}$ given above is an empirical function that has been found to best fit the experimental data. The theoretical model of the relationship between the conductivity and

Table 3
Parameters for the steady-state conductivity of a Nafion membrane (N-211) containing various compositions of ammonium ions at 80 °C. These parameters are based on a fit of experiment data given in Fig. 4(a and b) in Ref. [27].

RH (%)	A_1	A_2	A_3	A_4
30	0.119	9.01	13.13	0.21
40	0.070	8.81	19.62	0.50
50	0.088	8.11	30.95	2.21
60	0.046	8.59	36.89	5.10
70	0.068	7.64	50.30	10.34
80	0.159	6.12	71.97	19.05
90	0.541	4.66	125.08	32.68
100	9.989	3.54	1154.38	52.95

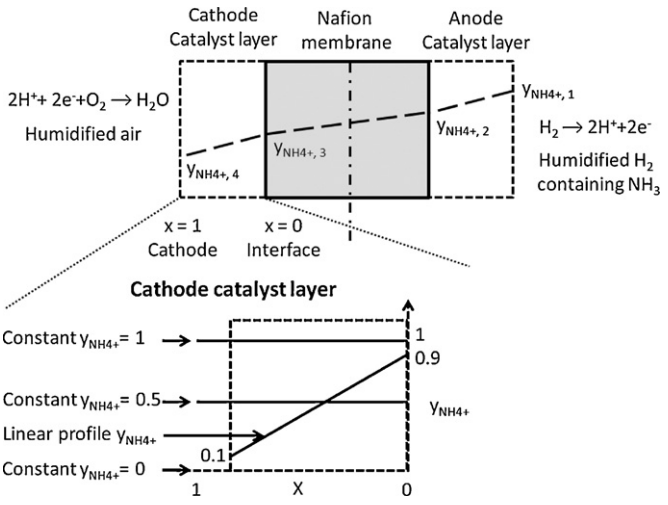

Fig. 4. 1D schematic of an ammonium contaminated MEA.

$y_{NH_4^+}$ has already been discussed in our previous work [27].

Since ammonia is introduced at the anode as an impurity in H_2, ammonia adsorption on Nafion starts at the contacted interface before it is transported to the cathode, causing some potential gradients in ammonium composition within an MEA, see Fig. 4. As mentioned in the introduction, ammonium transport through a membrane having thickness 10–100 μm is relatively fast [4]. Consequently, during fuel cell operation, the ionic conductivity of both anode and cathode catalyst layer would be adversely affected by the displacement of protons by ammonium cations [7]. If the ammonium distribution throughout an active catalyst layer is known, the overall effective conductivity ($\sigma_{\text{overall cat}}$) can be obtained by integrating the conductivity throughout that layer. However, to date, there has been no study that has ever investigated the concentration profile of proton-containing cations (i.e., ammonium ions) in both the membrane and the catalyst layer of a PEMFC. Only a few studies have reported the concentration profile of nonproton-containing cationic ions (i.e., metal cations) within a polymer membrane during fuel cell operation [39–41]. They have suggested that, at the steady-state operation, the distribution of contaminant ions depends strongly on the operating conditions (i.e., temperature, humidity, current density, etc.), concentration of contaminant cations in a fuel and/or oxidant stream, properties of cations (i.e., charge), type of polymer ionomer, and physical properties of the catalyst layer (i.e., polymer loading, porosity, etc.) [39,41]. This is because these operating parameters affect the kinetics of cationic adsorption at the anode, ion transport, and cationic removal at the cathode. It is expected that these operating parameters would affect an ammonium-contaminated fuel cell operation in a similar way. However, a detailed investigation of the ammonium concentration distribution within the anode and cathode layer during fuel cell operation is beyond the scope of this study.

In Fig. 4, two possible constant concentration profiles of ammonium ions in an active layer (with $y_{NH_4^+} = 0$ or 1) are shown, which represent the best and worst situation for fuel cell operation, respectively. For a partially contaminated catalyst layer, the linear concentration profiles of the cathode layer with $y_{NH_4^+} = 0.9 - 0.8x$ and $y_{NH_4^+} = 0.5$, respectively, were adopted for comparison in an explicit manner in this work. These two profiles yield the same average ammonium content ($y_{NH_4^+} = 0.5$) in the catalyst layer. The expressions for the calculation of overall conductivity of a contaminated catalyst layer are shown as follows:

$$\sigma_{\text{overall cat}} = \int_0^1 \sigma_{eff}^{cat}\, dx \quad (10)$$

Table 4
Parameters for conductivity modelling in the cathode catalyst layer.

Parameter	Value	Reference
r_{agg}	40 nm[a]	[44]
δ	1.9 nm[a]	[44]
ε_{agg}	0.17[a]	[44]
ε_{cat}	0.3–0.5	[28,31,32,43]

[a] The ionomer loading was 47.4 wt.% on a carbon support (Ketjen black (KB)).

assuming $\sigma_{eff}^{cat} = C\sigma_{yNH4+}$ where

$$C = (1-\varepsilon_{cat})\left[1+\frac{(\varepsilon_{agg}-1)}{(1+(\delta/r_{agg}))^3}\right]$$

$$\sigma_{yNH4+} = F_1^n(y_{NH4+}) \quad (11)$$

$$y_{NH_4^+} = F_2^n(x) \quad (12)$$

$$\sigma_{\text{overall cat}} = (1-\varepsilon_{cat})\left[1+\frac{(\varepsilon_{agg}-1)}{(1+(\delta/r_{agg}))^3}\right]\int_0^1 \sigma_{y_{NH_4^+}}\,dx \quad (13)$$

where x is the normalized distance from the membrane interface/catalyst layer in the x-dimension; $F_1^n(y_{NH_4^+})$ is the correlation between the conductivity as a function of $y_{NH_4^+}$ as shown in Eq. (9); and $F_2^n(x)$ is the ammonium distribution within the catalyst layer as a function of x.

The expression Eq. (13) can be used to estimate the overall conductivity of the active layer both at anode and cathode. However, most of the studies have investigated only the physical properties of the cathode catalyst layer because in the absence of impurity, the performance of a fuel cell is mainly limited by the kinetics of oxygen reduction and/or efficiency of proton transport processes at the cathode [3,42]. The parameters for the constant factor C at the anode are, thus, not available in the literature, but should be similar to those at the cathode. In this study, we have demonstrated how to predict the overall conductivity of an ammonium-contaminated cathode layer at typical fuel cell conditions using the modified agglomerate model (Eq. (13)). A typical set of model parameters for the effective conductivity calculation at the cathode are given in Table 4. However, it can be seen that the reported value for ε_{cat} varies significantly from 0.3 to 0.5 [28,31,32,43]. This parameter depends strongly on the support material, Pt loading, Nafion loading, preparation method, etc. In this work, we use an average value (ε_{cat} = 0.4) to estimate the effective conductivity at the cathode. The expression for the effective conductivity (Eq. (6)) at the cathode operating at various humidities and 80 °C can be simplified to:

$$\sigma_{\text{eff},y_{NH_4^+}}^{\text{cathode}} = 0.167\sigma_{y_{NH_4^+}} \quad (14)$$

$$\sigma_{\text{overall cat}}^{\text{cathode}} = 0.167\int_0^1 \sigma_{y_{NH_4^+}}\,dx \quad (15)$$

where $\sigma_{\text{eff},y_{NH_4^+}}^{\text{cathode}}$ and $\sigma_{\text{overall cat}}^{\text{cathode}}$ are the effective conductivity in the cathode catalyst layer and the overall conductivity of the cathode catalyst layer, respectively; $\sigma_{y_{NH_4^+}}$ is the conductivity of an ammonium-poisoned Nafion polymer (N-211) at a given $y_{NH_4^+}$ and %RH at 80 °C (Eq. (9)).

3.5. Prediction of the ionic conductivity of Nafion ionomer in the catalyst layer

Due to the lack of direct measurements of the conductivity of a poisoned catalyst layer, the accuracy of our predicted effective conductivity was validated using the experimental conductivity of an uncontaminated catalyst layer and the percentage of performance degradation of a fully ammonium-poisoned PEMFC.

In Fig. 5, the unfilled circles indicate the experimental conductivity at various humidities and 80 °C of an uncontaminated catalyst layer determined by a hydrogen pump technique employed by Iden et al. [44] and the dashed line represents a fit of their data. The solid line shows the predicted conductivity of the cathode catalyst layer ($\sigma_{\text{overall cat}}^{\text{cathode}}$) calculated from Eq. (15) using $y_{NH_4^+} = 0$. It can be seen that in the absence of impurities, the predicted values agree extremely well with experimental data. The estimated percentage decrease of the $\sigma_{\text{overall cat}}^{\text{cathode}}$ of the fully ammonium-poisoned PEMFC (constant $y_{NH_4^+} = 1$, dashed-dotted line in Fig. 5) was compared with the results of performance testing reported by Uribe et al. [7]. They studied the impact of ammonia on PEMFC performance, operating at 80 °C. A PEMFC was exposed to 30 ppm of NH_3 for 15 h, which was enough for complete neutralization of the protonic sites of the MEA [45]. They found that the cell voltage decreased ca. 49–77% at current densities of 0.2–0.4 A cm^{-2}. In their study, we considered that the operating humidities at anode and cathode were both 100% and the Nafion ionomer in the cathode was in the fully NH_4^+-form. At this condition, it can be seen in Fig. 5 that the estimated overall cathode conductivity ($\sigma_{\text{overall cat}}^{\text{cathode}}$) of the Nafion ionomer in the fully NH_4^+-form was ca. 64% lower than that of the fully H^+-form, which corresponds well with the performance loss in a PEMFC [7]. Although only the estimated $\sigma_{\text{overall cat}}^{\text{cathode}}$ and the estimated percentage decrease in $\sigma_{\text{overall cat}}^{\text{cathode}}$ for the case of constant $y_{NH_4^+} = 0$ and 1, respectively, can be shown to be matched with experimental results (due to the lack of appropriate experimental data in the literature), the overall conductivity at the cathode layer for other cases should be able to be reasonably predicted. In Fig. 5, the estimated $\sigma_{\text{overall cat}}^{\text{cathode}}$ for the partially ammonium-contaminated cathode catalyst layer having a non-homogeneous profile (linear profile, average $y_{NH_4^+} = 0.5$) can be seen to be slightly higher than that with a homogeneous profile ($y_{NH_4^+} = 0.5$) with the same equivalent ammonium content in it. Also, it is obvious that the estimated $\sigma_{\text{overall cat}}^{\text{cathode}}$ of the catalyst layer with various $y_{NH_4^+}$ constant profiles varies considerably with humidity (30–100%RH). The predictions suggest that the effect of ammonium content on $\sigma_{\text{overall cat}}^{\text{cathode}}$ is more significant than the ammonium ion distribution in the catalyst layer. Fig. 6 shows the effect of position on the predicted $\sigma_{\text{eff},y_{NH4+}}^{\text{cathode}}$ for a catalyst layer having a linear ammonium distribution profile ($y_{NH_4^+} = 0.9 - 0.8x$, average $y_{NH_4^+} = 0.5$). It can be seen that the influence of humidity on the conductivity is also very significant.

Since the rate of ammonia removal at the cathode is relatively slow compared to the rate of ammonia uptake [5,7], it is highly

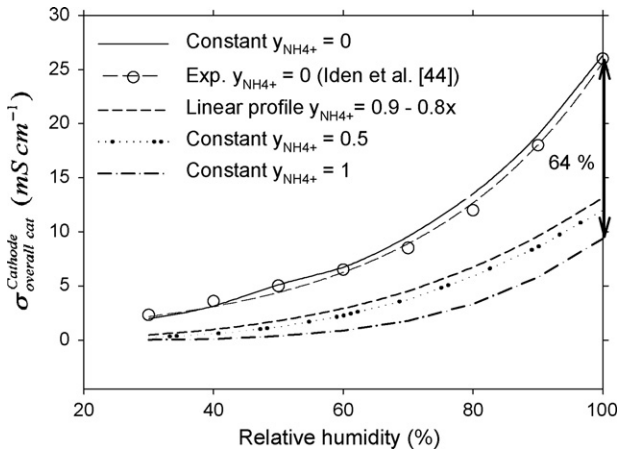

Fig. 5. Predicted $\sigma_{\text{overall cat}}^{\text{cathode}}$ of an ammonium-contaminated cathode catalyst layer having various ammonium concentration profiles as a function of relative humidity at 80 °C. ($\sigma_{\text{overall cat}}^{\text{cathode}}$ was obtained from Eq. (15).)

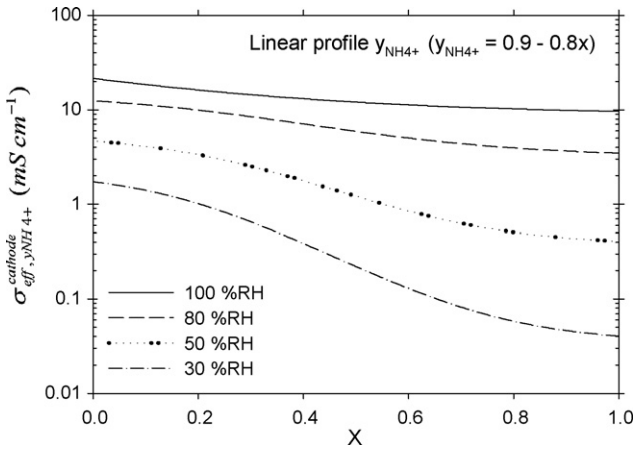

Fig. 6. Predicted $\sigma^{cathode}_{effl\,y_{NH_4^+}}$ conductivity as a function of position in an ammonium-contaminated cathode catalyst layer having ammonium distribution profile $y_{NH_4^+} = 0.9 - 0.8x$ (average $y_{NH_4^+} = 0.5$) at various humidities and 80 °C. ($\sigma^{cathode}_{effl\,y_{NH_4^+}}$ was obtained from Eq. (14).).

possible that the accumulation of ammonia in a PEMFC occurs over time. The predictions in Figs. 5 and 6 suggest that at some certain ammonium ion compositions in an active layer of a PEMFC and at some operating conditions (i.e., temperature, humidity, current density, concentration of ammonia in fuel gas and/or air stream, etc.), the impact of ammonia on ionic transport through the catalyst layer (proton depletion or proton starvation) can be significant enough to influence the overall fuel cell performance.

4. Conclusions

In our previous work [27], the effect of ammonia on ionic conductivity and esterification activity of a Nafion membrane (N-211) was studied. It was found that ammonia influences conductivity and esterification activity similarly under similar conditions. This is because both the conductivity and the esterification activity have a linear relationship with the number of proton/acid sites. In those studies, we demonstrated the relationship between the ionic conductivity and the esterification activity, this latter being able to predict the conductivity of a Nafion membrane (N-211).

In this study, proton availability of Nafion impregnated on a carbon support and Pt/C (30-Nfn/C and 30-Nfn/Pt/C) as used in typical fuel cells was explored using the same characteristic acid-catalyzed reaction (esterification of acetic acid with methanol) at various conditions (30–95%RH, 80 °C, and 1 atm). It was found that, under all the conditions studied, the esterification activity (r_{MeOAc}) on the supports was negligible and the esterification occurred only on the free proton/acid sites of the Nafion component. In the presence of 20 ppm NH_3/H_2, the esterification activity of supported Nafion decreased linearly with the ammonia uptake of a Nafion component under the same conditions. The results suggest that esterification can be used to quantitatively investigate the proton composition (y_{H^+}) of a Nafion component during exposure to ammonia or other potential impurities. The information of y_{H^+} gained from esterification was further used to estimate the overall conductivity of a catalyst layer using the modified agglomerate model and the correlation between conductivity and ammonium ion content ($y_{NH_4^+}$). The estimated effective conductivities of a cathode catalyst layer ($\sigma^{cathode}_{ovrall\ cat}$) was validated with the available literature data at two extreme conditions (non-poisoned [44] and fully ammonium-poisoned [7]). It was found that, under similar conditions, the $\sigma^{cathode}_{ovrall\ cat}$ for neat fuel cell operation and the percentage decrease in the $\sigma^{cathode}_{ovrall\ cat}$ of a fully ammonium-poisoned PEMFC matched well with experimental results reported in the literature [7,44]. Therefore, the predicted $\sigma^{cathode}_{ovrall\ cat}$ of an ammonium-contaminated active layer at other conditions using the same methodology should be reasonably accurate. The prediction suggests that under some operating conditions, especially at low humidity and high ammonium content, the durability and performance of PEMFC could be detrimentally impacted by proton depletion within the ionomer in the catalyst layer. This study showed that the characterization reaction also has the potential to be applied to quantitatively examine the number of proton/acid sites of other proton conducting materials impregnated on other supports (e.g., carbon, Pt/C, alloyed Pt/C) for a PEMFC under a wide range of conditions. Esterification provides us an easy means to study the impurity resistance of an ionomer component (in membrane form or on catalyst supports) without MEA fabrication, fully-equipped fuel cell testing, and also allows us to isolate the effect of impurity on the ionomer phase from that on the metal catalyst in an MEA. The combination of the esterification technique and the modified agglomerate model proposed in this work should provide helpful information for future investigations of impurity resistance of all sorts of proton conducting electrolytes, catalyst layer optimization, and computation modelling of PEMFC performance.

Acknowledgements

This research was financially supported by the U.S. Department of Energy (Award No. DE-FG36-07GO17011). K.H. would like to thank Dr. Kaewta Suwannakarn, Michael E. DeWitt, Jr., and Jack Z. Zhang for helpful discussions.

References

[1] K.C. Neyerlin, W.B. Gu, J. Jorne, H.A. Gasteiger, J. Electrochem. Soc. 154 (7) (2007) B631.
[2] L. Yuxiu, W.M. Michael, R.B. Daniel, G. Wenbin, J. Chunxin, J. Jacob, A.G. Hubert, J. Electrochem. Soc. 156 (8) (2009) B970.
[3] D.T. Song, Q.P. Wang, Z.S. Liu, T. Navessin, M. Eikerling, S. Holdcroft, J. Power Sources 126 (1/2) (2004) 104.
[4] R. Halseid, M. Heinen, Z. Jusys, R. Jürgen Behm, J. Power Sources 176 (2) (2008) 435.
[5] R. Halseid, P.J.S. Vie, R. Tunold, J. Power Sources 154 (2) (2006) 343.
[6] H.J. Soto, W.K. Lee, J.W. Van Zee, M. Murthy, Electrochem. Solid State Lett. 6 (7) (2003) A133.
[7] F.A. Uribe, S. Gottesfeld, T.A. Zawodzinski, J. Electrochem. Soc. 149 (3) (2002) A293.
[8] A.P. Saab, F.H. Garzon, T.A. Zawodzinski, J. Electrochem. Soc. 149 (12) (2002) A1541.
[9] C. Boyer, S. Gamburzev, O. Velev, S. Srinivasan, A.J. Appleby, Electrochim. Acta 43 (24) (1998) 3703.
[10] K. Hongsirikarn, X. Mo, J.G. Goodwin Jr., J. Power Sources 195 (11) (2010) 3416.
[11] Y.-H. Cho, S.J. Yoo, Y.-H. Cho, H.-S. Park, I.-S. Park, J.K. Lee, Y.-E. Sung, Electrochim. Acta 53 (21) (2008) 6111.
[12] J. Lee, J. Seo, K.K. Han, H. Kim, J. Power Sources 163 (1) (2006) 349.
[13] A. Caillard, C. Charles, D. Ramdutt, R. Boswell, P. Brault, J. Phys. D: Appl. Phys. (4) (2009) 045207.
[14] E.A. Ticianelli, C.R. Derouin, A. Redondo, S. Srinivasan, J. Electrochem. Soc. 135 (9) (1988) 2209.
[15] E.A. Ticianelli, C.R. Derouin, S. Srinivasan, J. Electroanal. Chem. 251 (2) (1988) 275.
[16] M.S. Wilson, S. Gottesfeld, J. Electrochem. Soc. 139 (2) (1992) L28.
[17] S.J. Lee, S. Mukerjee, J. McBreen, Y.W. Rho, Y.T. Kho, T.H. Lee, Electrochim. Acta 43 (24) (1998) 3693.
[18] G.C. Li, P.G. Pickup, J. Electrochem. Soc. 150 (11) (2003) C745.
[19] E.B. Easton, T.D. Astill, S. Holdcroft, J. Electrochem. Soc. 152 (4) (2005) A752.
[20] M.G. Santarelli, M.F. Torchio, Energy Convers. Manage. 48 (1) (2007) 40.
[21] R.R. Passos, V.A. Paganin, E.A. Ticianelli, Electrochim. Acta 51 (25) (2006) 5239.
[22] L. Guangchun, G.P. Peter, J. Electrochem. Soc. 150 (11) (2003) C745.
[23] W. Rachmady, M.A. Vannice, J. Catal. 192 (2) (2000) 322.
[24] Y.J. Liu, E. Lotero, J.G. Goodwin Jr., J. Catal. 243 (2) (2006) 221.
[25] B.B.J.A. Kolde, M.S. Wilson, T.A. Zawodzinki, S. Gottesfeld, in: S. Gottesfeld, G. alpert, A. Landgrebe (Eds.), The Electrochemical Society Proceedings Series, Pennington, NJ, PV 95-23, 1995, p. 193.
[26] S. Slade, S.A. Campbell, T.R. Ralph, F.C. Walsh, J. Electrochem. Soc. 149 (12) (2002) A1556.
[27] K. Hongsirikarn, J.G. Goodwin Jr., S. Greenway, S. Creager, J. Power Sources 195 (1) (2010) 30.

[28] C.Y. Du, P.F. Shi, X.Q. Cheng, G.P. Yin, Electrochem. Commun. 6 (5) (2004) 435.
[29] K.M. Yin, J. Appl. Electrochem. 37 (8) (2007) 971.
[30] C.C. Boyer, R.G. Anthony, A.J. Appleby, J. Appl. Electrochem. 30 (7) (2000) 777.
[31] F. Jaouen, G. Lindbergh, G. Sundholm, J. Electrochem. Soc. 149 (4) (2002) A437.
[32] S. Kamarajugadda, S. Mazumder, J. Power Sources 183 (2) (2008) 629.
[33] Z.T. Xia, Q.P. Wang, M. Eikerling, Z.S. Liu, Can. J. Chem. Revue Canadienne De Chimie 86 (7) (2008) 657.
[34] D. Harvey, J.G. Pharoah, K. Karan, J. Power Sources 179 (1) (2008) 209.
[35] M. Secanell, B. Carnes, A. Suleman, N. Djilali, Electrochim. Acta 52 (7) (2007) 2668.
[36] M. Secanell, K. Karan, A. Suleman, N. Djilali, Electrochim. Acta 52 (22) (2007) 6318.
[37] F. Jaouen, G. Lindbergh, K. Wiezell, J. Electrochem. Soc. 150 (12) (2003) A1711.
[38] W. Sun, B.A. Peppley, K. Karan, Electrochim. Acta 50 (16/17) (2005) 3359.
[39] B.L. Kienitz, H. Baskaran, T.A. Zawodzinski Jr., Electrochim. Acta 54 (2009) 1671.
[40] T. Okada, J. Electroanal. Chem. 465 (1) (1999) 18.
[41] T.A. Greszler, T.E. Moylan, H.A. Gasteiger, Handbook of Fuel Cells, Wiley, 2009.
[42] F.H. Garzon, F.A. Uribe, Handbook of Fuel Cells, Wiley, 2009.
[43] Q. Wang, M. Eikerling, D. Song, Z. Liu, J. Electroanal. Chem. 573 (1) (2004) 61.
[44] H. Iden, A. Ohma, K. Shinohara, J. Electrochem. Soc. 156 (9) (2009) B1078.
[45] A. Uribe, Private communication, 2009.